Fatigue of plain concrete in uniaxial tension and in alternating tension-compression loading

Autor(en): **Cornelissen, H.A.W. / Reinhardt, H.W.**

Objekttyp: **Article**

Zeitschrift: **IABSE reports = Rapports AIPC = IVBH Berichte**

Band (Jahr): **37 (1982)**

PDF erstellt am: **17.09.2024**

Persistenter Link: https://doi.org/10.5169/seals-28920

Fatigue of Plain Concrete in Uniaxial Tension and in Alternating Tension-Compression Loading

Essais de fatigue sur du béton non armé, soumis soit à une tension de traction uni-axiale soit à une tension alternée de traction-compression

Ermüdungsverhalten von unbewehrtem Beton unter zentrischer Zugschwell- und Zugdruckwechselbelastung

H.A.W. CORNELISSEN
Dr. Ir.
Delft University of Technology
Delft, the Netherlands

H.W. REINHARDT
Prof. Dr.-Ing.
Delft University of Technology
Delft, the Netherlands

SUMMARY
Uniaxial repeated tension and tension-compression tests on plain concrete are described. The results are presented in S—N lines and in a modified Goodman diagram. By means of a statistical treatment the influence of scatter of the static strength on the fatigue results was ascertained. It is shown that the secondary cyclic creep velocity as well as the cyclic creep itself are criteria for the life of concrete.

RESUME
Les auteurs décrivent des essais qui montrent la performance du béton non armé, soumis à des tensions uni-axiales répétées soit en traction soit à des tensions qui varient de compression en traction. Les résultats sont représentés sous forme de courbes S—N, et de diagramme modifié de Goodman. Au moyen d'un traitement statistique, on arrive à mettre en évidence l'influence de la dispersion de la résistance statique sur les résultats d'essais de fatigue. Il est démontré que sous charges variables aussi bien la vitesse de fluage secondaire que le fluage même sont des critères pour la durée de vie du béton.

ZUSAMMENFASSUNG
Zentrische Zugschwell- und Zugdruckwechselversuche an unbewehrtem Beton werden beschrieben. Die Ergebnisse werden in Wöhlerlinien und einem Goodman-Diagramm wiedergegeben. Mit Hilfe statistischer Auswertung konnte der Einfluss der Streuung der statischen Festigkeitswerte auf die Ergebnisse der Ermüdungsversuche angegeben werden. Es wird gezeigt, dass die zeitliche Zunahme des sekundären Kriechens und ebenso das Ermüdungskriechen selbst als Bruchkriterium verwendet werden kann.

1. INTRODUCTION

With the advent of offshore concrete platform construction and the increasing interest in partially prestressed concrete, much attention has been focused on the fatigue behaviour of concrete. This interest concerns concrete structures as a whole, but also the constituent materials.
Whereas the behaviour of plain concrete under repeated compressive loading has been extensively studied in recent years, results concerning the behaviour in alternating tension and especially in tension-compression are relatively scarce. Results of tensile fatigue strength have been obtained in bending tests [1] or splitting tests [2]. Also, alternating splitting tension-compression was obtained by the application of compressive prestress [3]. A difficulty inherent in the above-mentioned test methods is that the stress distribution in the specimen is not sufficiently known during the course of the experiment, because stress is calculated from strain with linear theory of elasticity, assuming constant material properties. This actually is doubtful. To overcome these problems, experiments were set up where the specimens were loaded uniaxially. For that purpose a special testing machine was designed.
The aim of the investigations was to determine S-N diagrams (Wöhler-diagrams) for various stress levels. Furthermore a theoretical model was applied to fatigue, which could be used as a failure criterion.

2. EXPERIMENTS

2.1 Specimens and testing equipment

Constant amplitude tests at a frequency of 6 Hz were carried out on tapered cylindrical specimens (ϕ 120 x 300 mm^2). The concrete was composed of 325 kg/m^3 rapid-hardening Portland cement type B (according to The Netherlands Standard), 1942 kg/m^3 river gravel with maximum grain size of 16 mm. The water-cement ratio was 0.50. After a curing period of 14 days the specimens were stored in the laboratory ("drying specimens") or wrapped in plastic sheeting ("sealed specimens"). The specimens were tested in the fifth week after casting.
For applying the load, steel platens were glued to the top and bottom of the cylinders. A special gluing press was used to provide plane-parallel and axial connection of these platens. The specimens were mounted in the testing machine

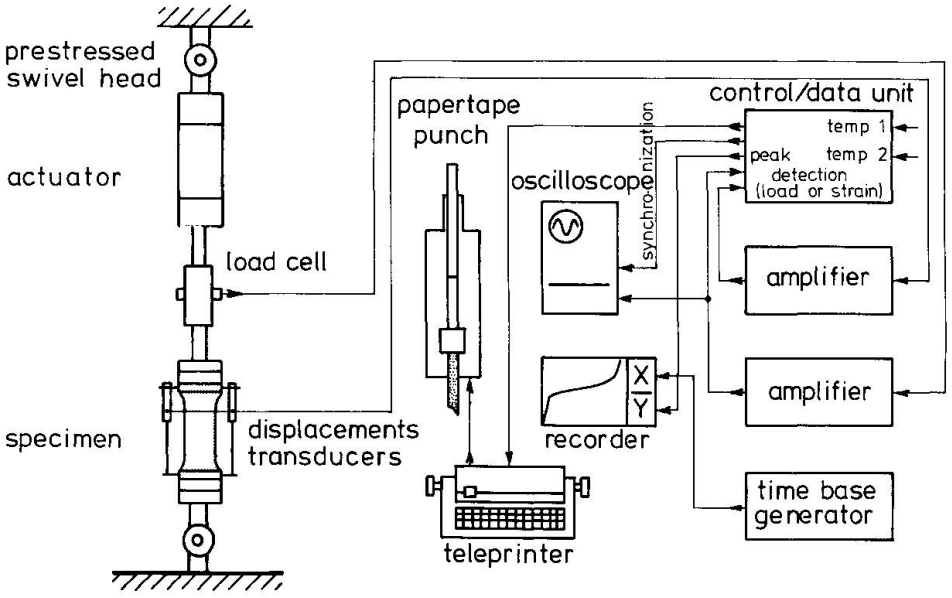

Fig. 1 Loading and controlling system (schematic)

by means of bolted connections. The frame of this machine consisted of standard steel beams. To achieve axial loading the specimen was was placed between two swivel heads, provided with prestressed spherical bearings, to obtain a continuous loading signal in the compression-tension tests. The capacity of the dynamic actuator was 100 kN for both tension and compression. A schematic view of the loading system is presented in Fig. 1. The control and recording devices are also indicated there. By means of the control/data unit a sinusoidal loading signal was generated in such a way that the adjusted levels of the cyclic loading were reached in 6 cycles. During the dynamic tests the magnitudes of the loading as well as of the axial deformations were measured eight times per cycle and were stored in the memory of the control/data unit. Only the results of two subsequent cycles after continually increasing time intervals were stored and punched on paper tape. At failure the results of the preceding 50 cycles became available.
Because the development of the deformation (creep, expansion) is strongly dependent on the temperature, an environmental chamber was placed around the specimen. The average temperature was 21 ^{o}C ($\pm$ 0.2 ^{o}C) and the relative humidity 40-45%. The grips were also cooled in order to prevent heat transmission from the actuator to the specimen (see Fig. 2).

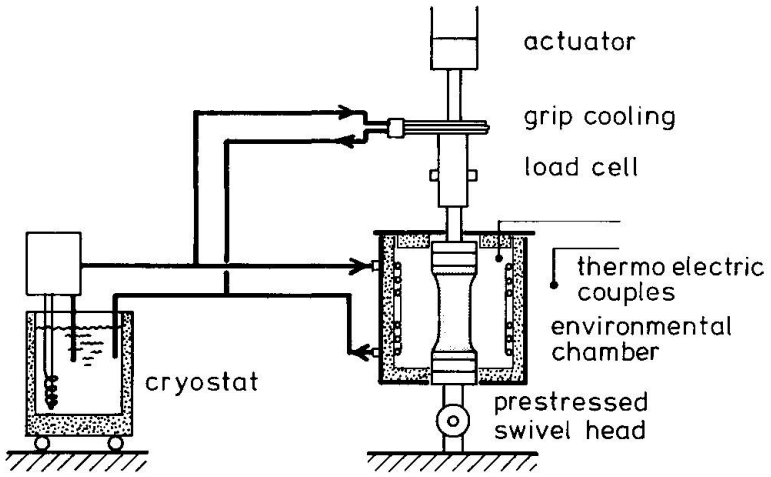

Fig. 2 Temperature control equipment

2.2 Adjustment of stress-strength levels of the dynamic loading signal

The upper and lower levels of the cyclic loading were taken as percentages of the static strength, which was estimated from the average results of static tensile and static compressive tests on specimens from the same concrete batch as the "dynamic" specimen. The static tensile strength was measured in a load-controlled test (0.10 N/mm^{2}s) on 5 or 6 tapered specimens. The compressive strength was determined on 3 standard cubes (150 mm^3) at a loading rate of 0.47 N/mm^{2}s.

3. RESULTS OF STATIC TESTS

The results of the static tensile and the static compressive tests, as well as the results of the control splitting tests om 150 mm cubes, are given in Table 1. In a later stage of the research program the σ-ε diagrams were recorded during the execution of the tensile tests. From these diagrams the Young's modulus (determinated as the secant modulus at 0.4 x f_{ct}) and the tensile strain (ε_1) at maximum tensile stress were taken. The average values are also presented in Table 1.

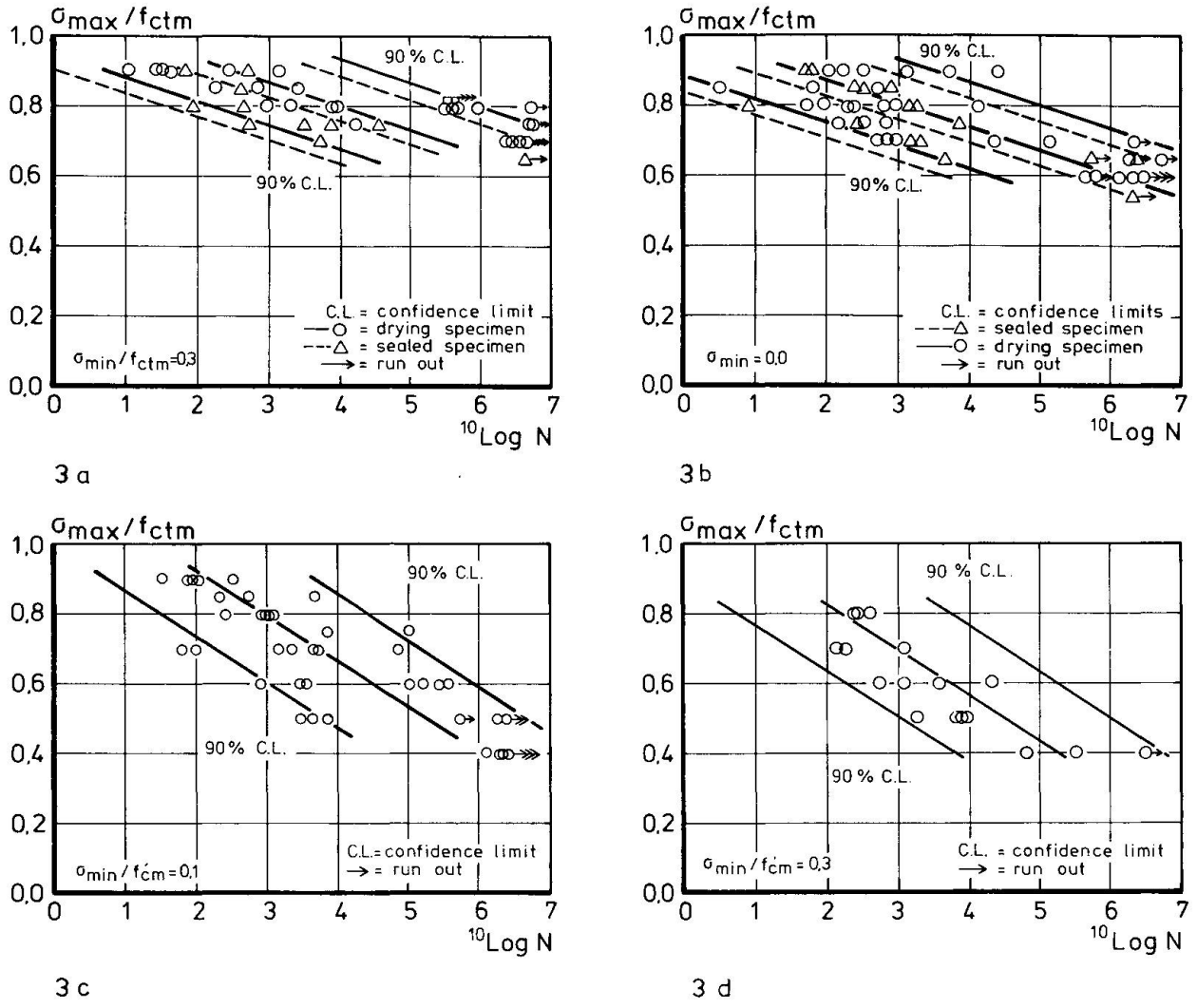

Fig. 3 S-N diagrams for dynamic tensile tests (a, b) and for tension-compression (c, d)

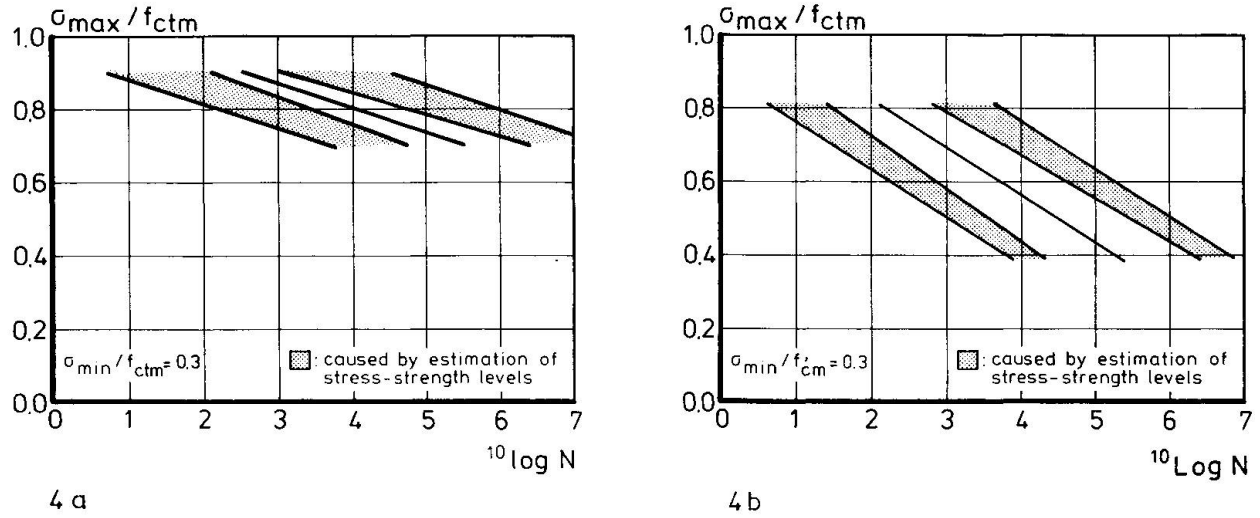

Fig. 4 Scatter in the S-N diagrams for tension (a) and tension-compression (b), as partly caused by variations of the stress-strength levels

Table 1 Average values of static test results

	compression	splitting	uniaxial tension			
	f'_{cm} N/mm²	f_{csplm} N/mm²		f_{ctm} N/mm²	E_{cm} N/mm²	ε_{1m} 10^{-6}
average value	47.5	2.83	"drying"	2.43	35870	96.3
			"sealed"	2.79	35390	123.3
average v%	3.6	7.5	"drying"	7.2	7.4	8.5
			"sealed"	3.7	8.4	8.4
k	50	50	"drying"	39	13	13
			"sealed"	9	9	9

note: k = number of concrete batches, each consisting of about 6 specimens, subjected to static tension, 6 for dynamic testing, 3 cubes for static compression and 3 for splitting tests.

4. RESULTS OF DYNAMIC TESTS

4.1 S-N diagrams

About 250 constant amplitude tests were executed with various combinations of lower and upper stress-strength levels. Six fixed lower levels were investigated, namely, 40, 30 and 20 per cent of f_{ctm}, 0 and 10, 20 and 30 per cent of f'_{cm}. In the various experiments the upper level varied from 40 to 90 per cent of f_{ctm}. For each lower level investigated, the test results are represented in S-N diagrams in which the number of cycles to failure is related to stress level parameters. Some typical examples are shown in Figs. 3a and 3b for dynamic tensile tests, and in Figs. 3c and 3d for alternating compression-tension. The lines drawn in these diagrams are the result of a multiple linear regression analysis. In this analysis tension and compression-tension were treated separately. Also it was decided to consider the maximum number of cycles of the "run-outs" as the number of cycles to failure. The following expressions were derived for drying specimens:

dynamic tensile tests ($\sigma_{min}/f_{ctm} \geq 0$):

$$^{10}\log N = 15.02 - 14.90 \cdot \frac{\sigma_{max}}{f_{ctm}} + 3.13 \cdot \frac{\sigma_{min}}{f_{ctm}} \qquad (1)$$

It turned out that the humidity (drying or sealed) was significant at the 95% level. For sealed specimens the constant term in (1) should be replaced by 14.29. In both conditions the 90% confidence regions were $^{10}\log N \pm 1.84$.

A similar expression is valid for:

dynamic compression-tension ($\sigma_{min}/f'_{cm} > 0.0$):

$$^{10}\log N = 9.46 - 7.71 \cdot \frac{\sigma_{max}}{f_{ctm}} - 3.78 \cdot \frac{\sigma_{min}}{f'_{cm}} \qquad (2)$$

The 90% confidence regions were estimated as $\log N \pm 1.45$.

It appears from formulas (1) and (2) that especially the maximum stress-strength level influences the number of cycles to failure. But also the lower level is important. An increase of this level in the case of compression, or a decrease of this level with respect to tension, results in shorter life.

4.2 Scatter of stress-strength levels

In dynamic tests the maximum and minimum stress levels have to be adjusted to target values, these being generally percentages of the static strength of the specimen to be tested. This static strength has to be estimated from static test results of other specimens from the same concrete batch, which results in deviating stress-strength levels and therefore scatter of the test results. To compare test results of different investigators, it is important to know what part of the scatter can be attributed to random errors of the adjusted stress-strength levels and what part is caused by the possible stochastic nature of fatigue. Moreover, in practice the scatter of static strength is often taken into account by means of characteristic strength (a lower limit of the strength distribution). When this strength is taken as the reference value, scatter in the unsafe direction of life will be mainly caused by the probability aspects of fatigue itself. In the following only a short description of the statistical treatment can be presented. Details of the approach can be found in [4]. In this approach the adjustments made to the maximum and minimum stress-strength levels are assumed to be the intended levels plus the error terms $\underline{h}_1$ for the maximum and $\underline{h}_2$ for the minimum. The distributions of the error terms are assumed to be normal with mean zero. The error terms have been incorporated in the following expression, which is valid for dynamic tension-compression.

$$\underline{^{10}\log N} = B_o + B_1\left(\frac{\sigma_{max}}{f_{ctm}} + \underline{h}_1\right) + B_2\left(\frac{\sigma_{min}}{f'_{cm}} + \underline{h}_2\right) + \underline{e} \qquad (3)$$

The underlining denotes stochastic quantities. The error term $\underline{e}$ reflects the total error minus $\underline{h}_1$ and $\underline{h}_2$.
It can be shown that $\underline{h}_1$ and $\underline{h}_2$ do not affect the expectation of $\underline{\log N}$, and therefore do not affect the position of the average S-N lines. On the contrary, the scatter of $\underline{\log N}$ will be influenced and can be expressed as follows:

$$\mathrm{var}(\underline{\log N}) = \{B_1^2\ \mathrm{var}\ \underline{h}_1 + B_2^2\ \mathrm{var}\ \underline{h}_2 + 2B_1B_2\ \mathrm{cov}(\underline{h}_1,\underline{h}_2)\} + \{\sigma_o^2\} \qquad (4)$$

in which: $\mathrm{var}\ \underline{h}_1 = v_t^2 \cdot \left(\frac{\sigma_{max}}{f_{ctm}}\right)^2$, $\mathrm{var}\ \underline{h}_2 = v_c^2 \cdot \left(\frac{\sigma_{min}}{f'_{cm}}\right)^2$

$$\mathrm{cov}(\underline{h}_1, \underline{h}_2) = v_t \cdot v_c \cdot \left(\frac{\sigma_{max}}{f_{ctm}}\right) \cdot \left(\frac{\sigma_{min}}{f'_{cm}}\right), \quad \sigma_o^2 = \mathrm{var}\ \underline{e}$$

v_t and v_c are the coefficients of variation of f_{ct} and f'_c respectively. It can be seen in (4) that the total variance of log N is subdivided into a part caused by erroneous adjustments of the stress-strength levels and a part caused by the stochastic nature of fatigue and the execution of the tests. This can also be demonstrated in the S-N diagrams. Two examples are given in Figs. 4a and 4b. It is shown that a considerable part of the scatter has its origin in the variability of the adjustments of the levels. Because of a better estimation of f'_c than f_{ct}, the scatter caused by the levels is smaller in the case of compression-tension. On the other hand, with respect to σ_o^2 (stochastic nature, execution of experiments), greater variation was found in tension-compression tests.

4.3 Goodman diagram

To show the interaction of various upper and lower stress ratios equations (1) and (2) have been evaluated. This has been done for combinations of maximum and minimum stress-strength levels using appropriate average values of log N. The calculated modified Goodman diagram is represented in Fig. 5. It can be observed that in the tension-compression part of the diagram there exists a discontinuity, especially for tests of long duration (lower maximum level), where the effect of compression may be more important. Whether or not this discontinuity is a sys-

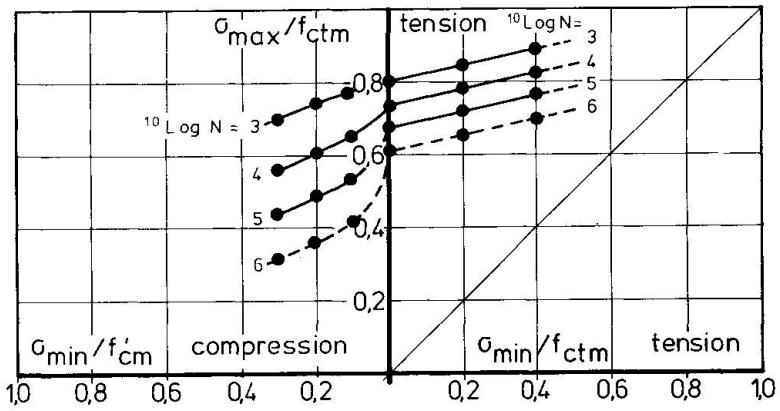

Fig. 5 Modified Goodman diagram for uniaxial tension and tension-compression

tematic phenomenon should be investigated in further experimental and theoretical work, where special attention should be paid to crack propagation and orientation.

5. THEORETICAL TREATMENT

5.1 A failure model applied to fatigue

A fracture mechanics approach was used by Wittmann and Zaitsev [5] to develop a theoretical model for the fracture behaviour of cement-based materials. This model was verified by short- and long-term tests. Now this model will be applied to the cyclic test results.
In a given material unstable crack propagation will occur when a critical crack length is reached. These critical crack length is assumed to be independent of the type and duration of the loading [5]. In [6] it has been deduced that the crack length S, at time t, can be expressed as:

$$S(t) = F\{C.M(t)\} \tag{5}$$

To a good approximation C is a material constant, and the function F has to be determined by numerical simulation methods and depends on the material configuration (pores, aggregates). The so-called measure of destruction M(t) can be derived from:

$$M(t) = \frac{\sigma(t)}{f_c(t)} \cdot \frac{1}{m(t)} \cdot \sqrt{\frac{E_c(t)}{E_c(t=0)} \cdot (1 + \phi(t))} \tag{6}$$

In this formula the creep coefficient $\phi(t)$ also represents creep at the crack tip and m(t) takes into account the effect pre-loading (stress-redistribution). For short-term tests to failure ($\sigma(t) = f_c(t)$), M(t) will be unity, because $\phi(t) = 0$ and m(t) as well as $E_c(t)/E_c(t=0)$ are equal to one. As stated before, at failure S(t) in formula (5) is independent of the type of test, and so are C and F. So for different test conditions M(t) = 1 at failure, so M can be regarded as a failure criterion.
With respect to the cyclic tests only the results with log N $\leq$ 6 have been analysed. It is therefore assumed, for these relatively short testing periods (< 48 hours), that m(t) = 1 and that the variations in the strength and in Young's modulus can be neglected. Equation (6) is thus simplified to:

$$M(n) = \frac{\sigma_{max}}{f_{ctm}} \cdot \sqrt{1 + \phi_{cycl}(n)} \tag{7}$$

$\phi_{cycl}(n)$ was calculated from the total peak strains in the tensile parts of the cycles (ε_{tot}) and the instantaneous strain (ε_i) at σ_{max} as determined from E_{cm}. A typcial relation between peak strain and n as well as the definition of the ultimate strain at failure are shown in Fig. 6. M at failure was calculated for

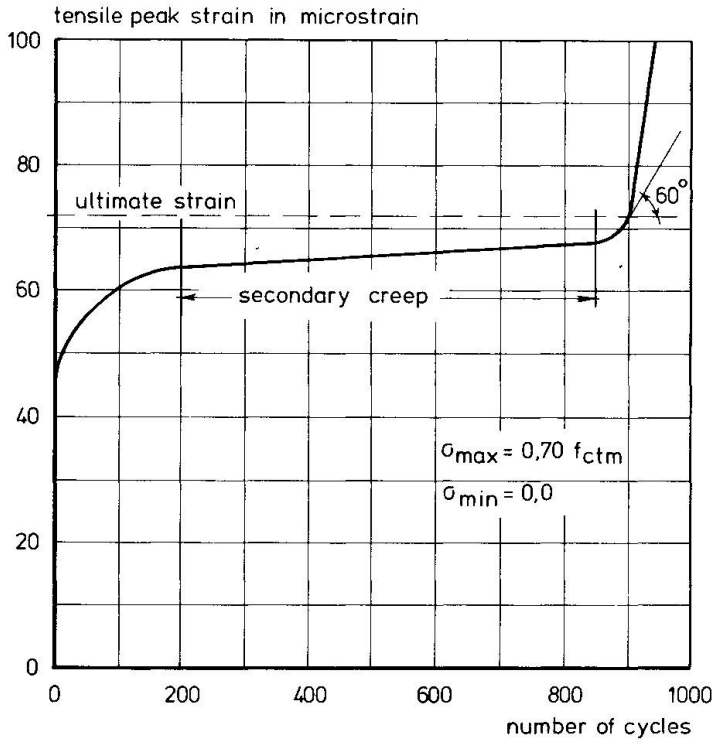

Fig. 6 Typical cyclic peak strain curve as measured on a "drying" specimen

68 dynamic tests. The average value was 1.02 (v = 9.8%). No significant difference was found between the "drying" and "sealed" specimens and between repeated tensile tests and tension-compression.
It can be concluded that with M as a failure criterion the magnitude of ϕ_{cycl} is an indication of the accumulated damage in the material. It can also be interpreted as a failure criterion which is based on maximum strain.

5.2 Secondary creep rate

Another approach to a failure criterion is the secondary creep which is almost constant during a long period of life (for definition see Fig. 6). A plot of the relation between log $\dot{\varepsilon}_{sec}$ and log N is shown in Fig. 7. This relation can be approximated by the following formula:

$$^{10}\log N = - 3.25 - 0.89\ ^{10}\log \dot{\varepsilon}_{sec} \qquad (\dot{\varepsilon}_{sec} \text{ per second}) \qquad (8)$$

No significant difference was found between "drying" and "sealed" specimens, nor between cyclic tension and tension-compression.
Formula (8) indicates that strain increase during life determines life. This was also found for tensile creep [7].
The approach adopted here has the additional advantage that it is independent of the stress and will therefore not be influenced by scatter of the stress-strength levels.

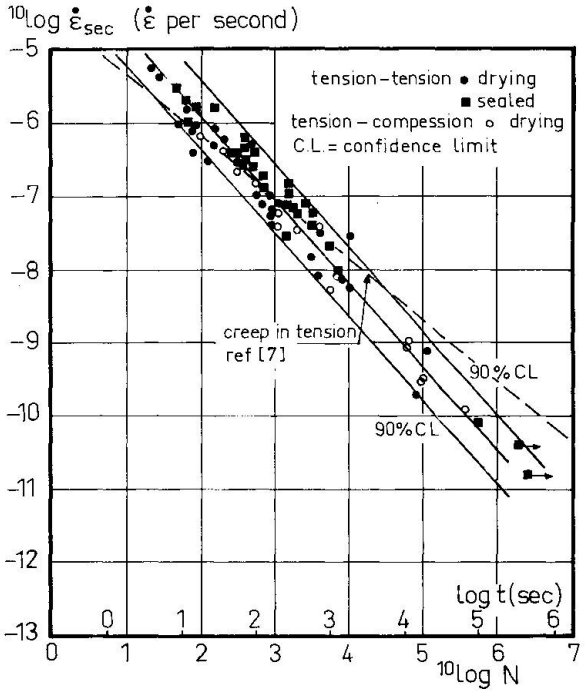

Fig. 7 Relation between the secondary creep velocity and life

6. CONCLUSIONS

The following conclusions can be drawn from this investigation:

S-N lines could be determined for various combinations of minimum (tension or compression) and maximum (tension) stress-strength levels.

By means of statistical methods the scatter of the test results in the S-N diagrams can be explained in part by the variability of the static strengths, causing random errors of the stress-strength levels

Although low minimum stress-compressive strength levels were applied in the dynamic compression-tension tests, a considerable decrease in the number of cycles to failure was found as compared with zero-tension tests. Alternation from compression to tension seems to cause additional damage

The magnitude of the theoretically deduced measure of destruction M is in good agreement with the experimental results

There exists a distinct relation between secondary creep velocity (at tensile peak stress) and the number of cycles to failure. The confidence region was found to be narrow.

7. NOTATION

E_c = Young's modulus (N/mm^2)
f_{ct} = static tensile strength (N/mm^2)

f'_c = static compressive strength (N/mm^2)
f_{cspl} = static splitting tensile strength (N/mm^2)
$---_m$ = indicates average value
n = number of cycles
N = number of cycles to failure
v = coefficient of variation
ϕ_{cycl} = cyclic creep coefficient, $(\varepsilon_{tot} - \varepsilon_i)/\varepsilon_i$
σ_{max}, σ_{min} = upper and lower limit of the dynamic stress
$\dot{\varepsilon}_{sec}$ = secondary creep rate at σ_{max} (per second).

8. ACKNOWLEDGEMENT

The authors wish to thank CUR-VB (Netherlands Committee for Research, Codes and Specifications) for the financial support.

9. REFERENCES

1. Raithby, K.D. Some flexural fatigue properties of concrete - effects of age and methods of curing. First Australian Conference on Engineering Materials, University of New South Wales, 1974, pp. 211-229.
2. Tepfers, R. Tensile fatigue strength of plain concrete. ACI-Journal, August 1979, pp. 919-933.
3. Tepfers, R. Fatigue of plain concrete subjected to stress reversals. ACI Fall convention, 1980, San Juan, Puerto Rico.
4. Cornelissen, H.A.W., Timmers, G. Fatigue of plain concrete in uniaxial tension and in alternating tension-compression. Experiment and results. Report no. 5-81-7. 1981, Stevin laboratory, Delft University of Technology, The Netherlands.
5. Wittmann, F.H., Zaitsev, Y.V. Verformung und Bruchvorgang poröser Baustoffe bei kurzzeitiger Belastung und Dauerlast. DAfStb Heft 232, 1974, pp. 65-145.
6. Zaitsev, Y.V., Scerbakov, E.N. Creep fracture of concrete in prestressed concrete members during manufacure. Fracture, 1977, vol 3, ICF4, Waterloo, Canada, pp. 1219-1222.
7. Nishibayashi, S. Tensile creep of concrete. Proc. Rilem Colloquium, Creep of Concrete, Leeds, Engeland 1978.